# All-optical manipulation of light in X- and T-shaped photonic crystal waveguides with a nonlinear dipole defect

Evgeny N. Bulgakov[1,2] and Almas F. Sadreev[1]
[1]*L.V. Kirensky Institute of Physics, 660036, Krasnoyarsk, Russia*
[2]*Siberian State Aerospace University, Krasnoyarsk, Russia*
(Received 16 May 2012; revised manuscript received 8 July 2012; published 15 August 2012)

We consider light transmission in X- and T-shaped photonic crystal waveguides which hold nonlinear defect with two resonant dipole modes. By use of the coupled-mode theory and by numerical solution of the Maxwell equations for the transverse-magnetic (TM) light mode, we show two stable types of the solutions. The first type has no cross talk, while the second type does owe to nonlinearity of the defect. We show also that direct path transmission processes in the waveguides play an important role for breaking of symmetry.

DOI: 10.1103/PhysRevB.86.075125 PACS number(s): 42.25.Bs, 42.65.Pc, 42.70.Qs

## I. INTRODUCTION

Microcavities or resonators formed by point defects and waveguides formed by line defects in photonic crystals (PhCs) have been subjects for plenty of research because of their capability to confine photons within a small volume, and they are expected to be key building blocks for miniature photonic functional devices and photonic integrated circuits. The point defect has a well-defined spectrum of discrete eigenfrequencies and corresponding localized eigenstates classified as monopole, dipole, etc., modes.[1] The eigenstates of the waveguide are extended with a continual spectrum of eigenfrequencies forming the propagation band for light. By exploiting the rich and well-defined orthogonal modes which provide abundant degrees of freedom for the choice of junctions (having different spectral mode overlap and frequency separation), a vast number of different functional light devices might be considered. A junction of point defect with the waveguide is the basic element. Therefore, symmetry selection rules for coupling of the localized states of the point defect with extended states of the waveguide play a fundamental role in the PhC devices. In particular, Johnson *et al.*[2] have shown that symmetry of the defect cavity dipole modes plays a decisive role for wave transmission in waveguide intersections. It was shown that cross talk in the X-shaped waveguide is eliminated due to the symmetry.

Thus, the role of nonlinearity is a key in the PhC devices because of the symmetry breaking. That phenomenon, with the establishment of one or more asymmetric states which no longer preserve the symmetry properties of the original state, is widely studied in the nonlinear optics with injection of input power.[3–12] The phenomenon of the symmetry breaking in analogy with the double-well potential[13] is realized in a nonlinear dual-core directional fiber.[14–16] Recently, the phenomenon was demonstrated in the most simple system of the directional waveguide coupled with two nonlinear defects, each presented by a single monopole resonant mode.[17–20] Yanik *et al.*[21] considered a nonlinear defect of elliptic shape at the center of the X-shaped photonic crystal (PhC) waveguide. They have shown that this system allows a control in one waveguide to switch the transmission of a signal on/off in another waveguide and that there is no energy exchange between the signal and the control, even in the nonlinear regime. Due to nonlinearity of the defect, the transmission over the $x$ direction can be reversibly switched on/off by a control power over the $y$ direction to realize an idea of an all-optical transistor in the X-shaped waveguide.

In this paper, we follow another aim to study the switching of on/off cross talk in the X- and T-shaped waveguides with the single defect cavity by use of a nonlinear coupling between dipole modes. We show that in this nonlinear system, there is the solution with no cross talk similar to the linear case.[2] An injected wave with definite parity excites only one dipole mode of that parity. However, we show that for swapping of light frequency or amplitude injecting light, there is a stable solution with dipole modes excited both irrespective to their parity to provoke cross talk.

## II. CMT THEORY OF X-SHAPED WAVEGUIDE

Let us consider the most symmetric case when a single nonlinear defect is disposed in the center of the PhC X-shaped waveguide as shown in Fig. 1. Each arm of the X-shaped waveguide supports the single band of guided TM mode spanning from the bottom band edge 0.315 to the upper one 0.41 in terms of $2\pi c/a$.[1,22] The TM mode has the electric field component parallel to the GaAs rods and is even with respect to the axis of the waveguide. Light propagated in the waveguide can excite only those eigenmodes of the defect rod cavity whose eigenfrequencies belong to the propagation band of the PhC waveguide. By choice of the defect rod's radius or dielectric constant, we can fit only the dipole eigenfrequencies into the propagation band of the waveguide.[1] Two degenerated bounded dipole modes $E_1(\mathbf{x})$ and $E_2(\mathbf{x})$ of the fully closed defect rod cavity are shown in Fig. 1. Henceforth, we call such a defect cavity a dipole defect. Furthermore, we remove two rows of the rods shown in Fig. 1 by open dashed circles in the orthogonal directions. That forms the X-shaped (cross) waveguide. However, we leave four rods around the defect rod in order to diminish the coupling of the dipole eigenmodes with continua of the waveguide. The way to make weak-coupling constants was used, for example, in Ref. 21. We define the defect rod at the center plus four rods around as the defect optical cavity. As a result, the dipole states become the extended resonant ones. Therefore, we can write for the electric field in the interior of the defect cavity[23,24]

$$E(x,y) = A_1 E_1(x,y) + A_2 E_2(x,y) + \tilde{\psi}(x,y), \qquad (1)$$

 

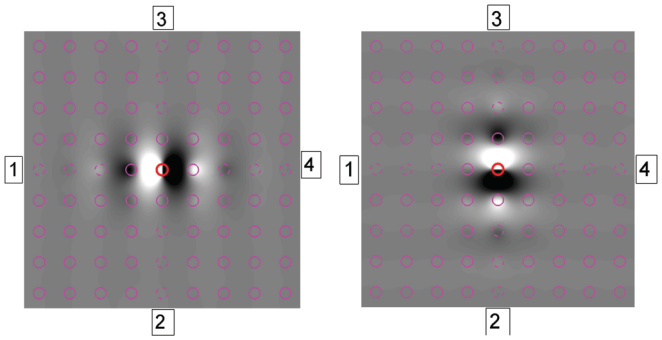


FIG. 1. (Color online) Two dipole eigenmodes $E_1$ and $E_2$, respectively, with the degenerated eigenfrequency $\omega_0 = 0.3763$ in the squared lattice PhC of GaAs dielectric rods with radius $0.18a$ and dielectric constant $\epsilon = 11.56$ where $a = 0.5$ $\mu$m is the lattice unit. These rods are shown by open pink circles. Removal of rods shown by dashed open pink circles forms the X-shaped PhC waveguide. The defect shown by an open circle has the radius $0.18a$ and $\epsilon_0 = 30$ and is positioned at the center of X-shaped waveguide. Numbers enumerate arms of the waveguide.

where the complex background function $\tilde{\psi}$ is a contribution of insignificant direct path nonresonant processes. We consider that the cavity defect rod is made from a Kerr medium, and that the dipole resonant frequencies are spaced far from the propagation band edges.

Following the coupled-mode theory[25] (CMT), we write the coupling matrix of the dipole modes with incoming waves in four arms of the waveguide as

$$D = \begin{pmatrix} \sqrt{\gamma} & 0 \\ 0 & \sqrt{\gamma} \\ 0 & -\sqrt{\gamma} \\ -\sqrt{\gamma} & 0 \end{pmatrix}, \quad \hat{\Gamma} = D^+ D/2 = \begin{pmatrix} \gamma & 0 \\ 0 & \gamma \end{pmatrix}, \tag{2}$$

where $\hat{\Gamma}$ is the decay matrix which is to be substituted into the CMT equations. Following Ref. 25 and the perturbation theory developed in Refs. 1 and 19, we write the following coupled-mode equations for the amplitudes of the dipole modes $A_m, m = 1,2$ as

$$\begin{aligned} [\omega - \omega_0 - V_{11} + i\gamma]A_1 - V_{12}A_2 &= i\sqrt{\gamma}(S_{1+} - S_{4+}), \\ -V_{12}A_1 + [\omega - \omega_0 - V_{22} + i\gamma]A_2 &= i\sqrt{\gamma}(S_{2+} - S_{3+}), \end{aligned} \tag{3}$$

where $S_{j+}, j = 1,2,3,4$ are the light amplitudes injected in the $j$th arm of the X-shaped waveguide. The matrix elements of perturbation theory

$$V_{mn} = -\frac{\omega_0}{2N_m} \int d^2\vec{r}\, \delta\epsilon(\vec{r}) E_m(\vec{r}) E_n(\vec{r}) \tag{4}$$

are a result of the contribution

$$\delta\epsilon(\vec{r}) = \frac{n_0 c n_2 |E(\vec{r})|^2}{4\pi} \approx \frac{n_0 c n_2 |A_1 E_1(\vec{r}) + A_2 E_2(\vec{r})|^2}{4\pi} \tag{5}$$

because of nonlinear change of the dielectric constant of the defect rod with instantaneous Kerr nonlinearity. $n_0 = \sqrt{\epsilon_0}$ and $n_2$ are the linear and nonlinear refractive indexes of the defect rod, respectively, and $c$ is the light velocity. Equation (5) implies the normalization of the eigenmodes as follows:[26]

$$N_m = \int d^2\vec{r}\, \epsilon_{\mathrm{PhC}} E_m^2(\vec{r}) = \frac{a^2}{cn_2} \tag{6}$$

with $\epsilon_{\mathrm{PhC}}$ as the dielectric constant of whole defect-free PhC. Because of symmetry, $N_1 = N_2$. After substitution of Eqs. (4) and (6), we write Eq. (3) in the dimensionless form

$$\begin{aligned} &[\omega - \omega_0 + \lambda_{11}|A_1|^2 + \lambda_{12}|A_2|^2 + i\gamma]A_1 + 2\lambda_{12}\mathrm{Re}(A_1^* A_2)A_2 \\ &\quad = i\sqrt{\gamma}(S_{1+} - S_{4+}), \\ &2\lambda_{12}\mathrm{Re}(A_1^* A_2)A_1 + [\omega - \omega_0 + \lambda_{22}|A_2|^2 + \lambda_{12}|A_1|^2 + i\gamma]A_2 \\ &\quad = i\sqrt{\gamma}(S_{2+} - S_{3+}), \end{aligned} \tag{7}$$

where

$$\lambda_{mn} = \frac{c^2 n_2^2}{a^2} \int_\sigma E_m^2(x,y) E_n^2(x,y) dx\, dy. \tag{8}$$

Here, the frequencies, the width, and the nonlinear constants are given in terms of $2\pi c/a$. Next, we have for the incoming and outgoing waves[25]

$$\begin{aligned} S_{1-} &= -S_{1+} + \sqrt{\gamma}A_1, \quad S_{2-} = -S_{2+} + \sqrt{\gamma}A_2, \\ S_{3-} &= -S_{3+} - \sqrt{\gamma}A_2, \quad S_{4-} = -S_{4+} - \sqrt{\gamma}A_1, \end{aligned} \tag{9}$$

the outgoing powers

$$P_j = |S_{j-}|^2, \tag{10}$$

and the transmissions

$$T_j = |S_{j-}|^2 \Big/ \sum_{i=1}^{4} |S_{i+}|^2. \tag{11}$$

We take the Kerr nonlinear refractive index $n_2 = 2 \times 10^{-12}$ cm$^2$/W. Other material parameters are listed in the caption of Fig. 1. By substituting numerically calculated eigendipole modes shown in Fig. 1 into Eqs. (4) and (5) with account of Eq. (6), we obtained $\lambda_{11} = \lambda_{22} = 1 \times 10^{-3}$, $\lambda_{12} = 3.5263 \times 10^{-4}$. The resonant width $\gamma$ was obtained directly from resonant transmission through PhC waveguide holding the linear dipole defect. The transmission was calculated by use of the Maxwell equations for the TM mode propagation, the procedure of which is described in Sec. III. As a result, we obtain $\gamma \approx 7.5 \times 10^{-4}$. Next, we consider different schemes of light injection into the X-shaped waveguide.

### A. Light injection into a single arm

Let the light be injected into the first arm, i.e., $S_{1+} \neq 0$, $S_{2+} = S_{3+} = S_{4+} = 0$. The self-consistent solutions of Eq. (7) are presented in Fig. 2. There are two types of solutions. For the first solution shown in Fig. 2 by dashed black lines, the even dipole mode is excited only. Respectively, we have no outgoing waves in the arms 2 and 3, i.e, cross talk is eliminated as was obtained by Johnson *et al.*[2] for the linear dipole defect cavity. The forward transmission $T_4$ has resonance behavior typical for the transmission in the waveguide coupled with a single mode of the nonlinear in-channel defect.[1,27] Furthermore, there is the solution with the even and odd modes excited both in some frequency domain as shown in Fig. 2(a) by the solid black line for the first even dipole mode and by the solid red line for the second odd dipole mode because of nonlinear coupling of the dipole modes in Eq. (7). Then, a participation of the odd dipole mode in light transmission gives rise to the outgoing waves in arms 2 and 3 as shown in Fig. 2(b). The outgoing waves have equal power, but the amplitudes are

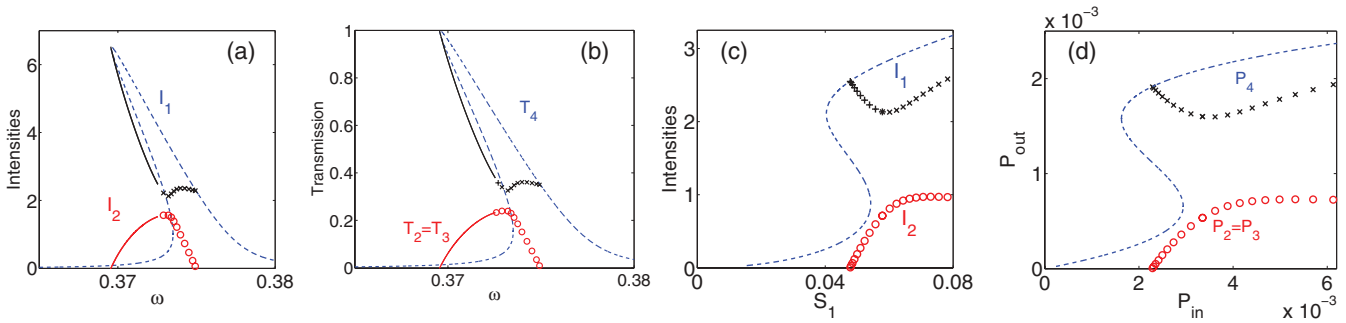


FIG. 2. (Color online) Frequency behavior of (a) intensities of the dipole modes $I_m = |A_m|^2$ and (b) light transmissions $T_j$ given by Eq. (11) when light is injected into the first arm for the fixed input amplitude $S_{1+} = 0.07$. The case of the first mode excited only is shown by the dashed blue line. The case of both modes excited is shown by solid lines or marked by crosses and open circles. (c) Intensities of the dipole modes as a function of input amplitude for fixed frequency $\omega = 0.374$. (d) Outputs vs input power. Domains of stability of the second solution with the even mode $E_1$ and odd mode $E_2$ excited both are marked by open circles and crosses.

opposite in the sign according to Eq. (9). The input-output power curves also demonstrate that these outgoing waves arise for the input power above the threshold as marked in Fig. 2(d) by open red circles. Thus, there are domains of stability in the space $\omega$ and $S_{1+}$ for cross talk.

We also inspected a stability of the solutions. We do not show the domain of stability of the first solution with the only excited dipole mode $E_1$. The second solution with both dipole modes excited is our prime interest. The domains of stability of this solution are marked in Fig. 2 and in all forthcoming figures by crosses and open circles. It is important to note that the domains of stability of both solutions over the input power coincide as seen from Fig. 2(d). Then, an application of light impulses will give rise to a bifurcation between the solutions, i.e., to the all-optical switching of cross talk.[12,17,18,28] Finally, following Ref. 19, we estimate the threshold for the incoming power $|S_{1+}|^2 \gtrsim \frac{\Gamma^2}{\lambda_{12}}$ where the second solution with symmetry breaking arises.

### B. Light injection into two arms

Let the light be injected into both arms with equal amplitudes. There are two choices. For the first one, light is injected into the neighboring arms, say, 1 and 2. That case has the mirror reflection symmetry with respect to a diagonal line between arms 1 and 2. The solutions of Eqs. (7) and (9) shown in Fig. 3 demonstrate breaking of this symmetry for the nonlinear dipole defect. For the symmetry-preserving solution, we have equal outputs in arms 3 and 4 as shown in Fig. 3 by dashed lines. For the symmetry-breaking solution marked by crosses and open circles, which is fully stable, the outputs are not equal. Moreover, there is selected frequency and selected value of the inputs at which the ratio of these outputs might be done extremely small, which gives us a possibility for the all-optical switching of outputs 3 and 4. Therefore, a single dipole nonlinear defect implied into the center of the X-shaped waveguide can give rise to the breaking of symmetry.

For the second choice, light is injected to the opposite arms 1 and 4. This way of injecting of light was proposed by Maes *et al.*[17,18] in the directional waveguide with two nonlinear monopole defects to establish breaking of the left/right symmetry. In Ref. 24, that result was obtained for the case of a single nonlinear dipole defect. For the present case of the X-shaped waveguide with the dipole defect in order, light may excite the dipole modes and the amplitudes of light are to have opposite signs in arms 1 and 4 as follows from Eq. (7). Results of the solution of the CMT equations (7) are shown in Fig. 4. There are two solutions. For the first solution with the even dipole mode $A_1$ excited only, there are no outgoing waves in the cross arms 2 and 3 (no cross talk) as shown in Fig. 4 by dashed lines. For the second solution with both dipole modes excited, cross talk occurs as shown in Fig. 4 by solid lines (unstable domain) or marked by open circles and crosses (stable domain). As follows from Eq. (9) irrespective to the solution, the outgoing waves in the cross arms 2 and 3 have equal intensities.

It is interesting to find out how the phase difference $\theta$ between input amplitudes into arms 1 and 4 affects the transmissions. One can see from Fig. 5 that the transmissions $T_1$ and $T_4$ are split as soon as $\theta \neq 0, \pi$ proportional $\sin\theta$. Moreover, we find stable solutions, which is remarkable by cross talk. In the vicinity of $\theta = \pi$, the cross outputs are almost

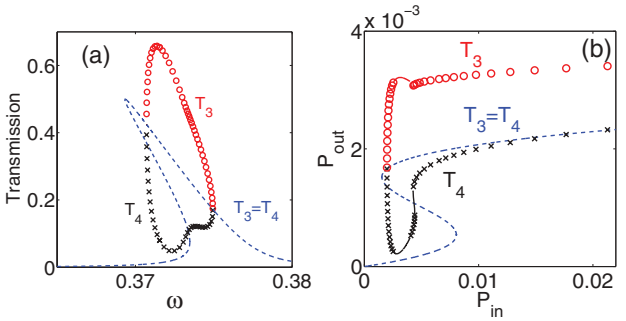


FIG. 3. (Color online) (a) Frequency behavior of light outputs to arms in the X-shaped waveguide for light injects into the first and the second arms with amplitudes $S_{1+} = S_{2+} = 0.05$. (b) Output power vs input power for $\omega = 0.372$. For the symmetry-preserving solution shown by dashed lines, we have equal transmissions $T_3 = T_4$ into arms 3 and 4. The stability of the symmetry-breaking solution is marked by open circles and crosses.

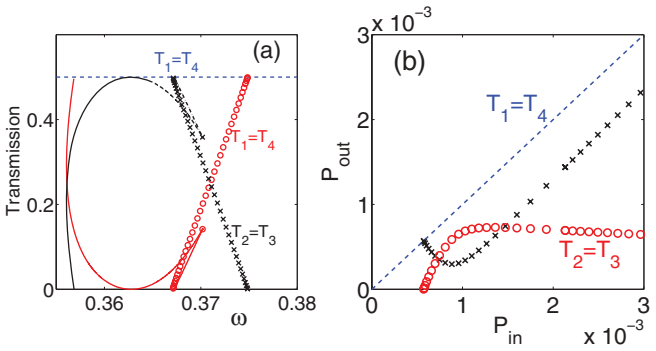


FIG. 4. (Color online) (a) Frequency behavior of light outputs to arms in the X-shaped waveguide for light injects into the first and the fourth arms with amplitudes $S_{1+} = -S_{4+} = 0.07$, respectively. (b) Outputs vs inputs for $\omega = 0.374$. The equal transmissions to arms 1 and 4 are shown by blue dashed lines. The stable solution with cross talk is marked by open circles and crosses.

constant around 92%. Thus, in that phase segment we obtain effective switching on/off of cross talk.

### C. Interference with direct path processes

As was shown in Sec. II A, injection of light into arm 1 might excite both dipole modes due to the nonlinearity of the dipole defect to give rise to cross talk. The outgoing waves in the cross arms have amplitudes that are opposite in sign but equal in the intensity. Now, assume light is incoming not only into arm 1 but also into arms 2 and 3 with $S_{2+} = S_{3+}$. Then, in arm 2, we have an interference of the the waves $t_{22} + t_{12}$ where $t_{22} = -S_{2+}$ because of the full reflection of the input waves injected into arms 2 and 3, and $t_{12}$ is the transmitted wave $1 \to 2$. In arm 3, we have similarly $t_{33} - t_{12}$ where $t_{33} = -S_{3+} = t_{22}$. Respectively, this results in symmetry breaking with respect to the mirror reflection of arms 2 and 3 provided that $t_{12} \neq 0$. Indeed, Figs. 6(a) and 6(b) demonstrate the symmetry-breaking phenomenon for that case.

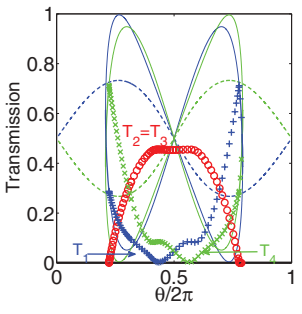


FIG. 5. (Color online) Transmissions for equal input power $|S_{1+}| = |S_{4+}| = 0.04$ into arms 1 and 4 for $\omega = 0.374$ as dependent on phase difference $\theta = \arg(S_{1+}) - \arg(S_{4+})$. The dashed thick lines show the stable transmissions to arms 1 and 4, which would have been even for the linear defect cavity. The solid lines show the solutions for the transmissions to arms 1 and 4, which are the result of nonlinearity of the defect but they are not stable. The stable domains of the solutions are marked by crosses, pluses, and open circles.

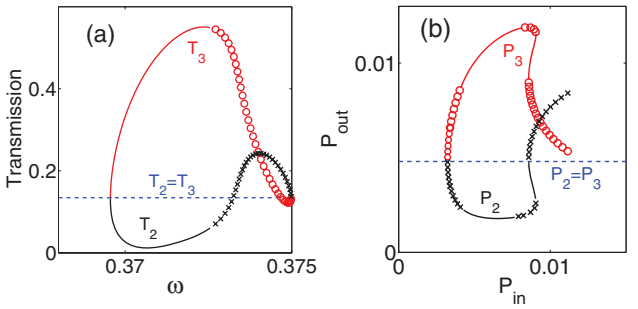


FIG. 6. (Color online) (a) Frequency behavior of light outputs to arms in the X-shaped waveguide for light injects into arm 1 $S_{1+} = 0.07$ and into arms 2 and 3 with $S_{2+} = S_{3+} = 0.03$. (b) Input-output curve for $\omega = 0.372$ and $S_{2+} = S_{3+} = 0.07$ for variation of the input into arm 1. Dashed line shows the stable symmetry-preserving solution with $T_2 = T_3$, while the dashed-dotted and solid lines show one of the symmetry-breaking solutions with $T_2 \neq T_3$. Open circles and crosses mark the domains of stability of the symmetry-breaking solution.

Instead of this complexity of inputs, which breaks the symmetry in respect to the outputs 2 and 3, we can take into account the direct path nonresonant processes in order to obtain similar results for injection into only arm 1. For example, in the PhC waveguide, light might directly path from input arm 1 into other arms of the X-shaped waveguide without excitation of the defect dipole modes. Therefore, the direct path processes can break the symmetry even for light injected into a single arm because of the Fano interference of the resonant transmission wave with the direct path wave. In order to take into account these direct path processes, we use generalized CMT (Ref. 25):

$$|S_-\rangle = C|S_+\rangle + D|A\rangle, \tag{12}$$

where the matrix $D$ is given by Eq. (2), the vectors $|S_\mp\rangle$ consist of four output/input amplitudes, respectively. Until now, we use $C = -1$, which means a transmission through only resonant modes of the defect cavity. However, if there are direct pathway nonresonant processes, then the matrix $C$ becomes nondiagonal:

$$C = \begin{pmatrix} a & b & b & c \\ b & a & c & b \\ b & c & a & b \\ c & b & b & a \end{pmatrix}. \tag{13}$$

Substitution of Eqs. (2) and (13) into the relation $CD^* = -D$ (Ref. 25) gives us

$$a = -1 + c, \quad b = i\sqrt{c(1-c)}, \tag{14}$$

where $1 \geqslant c \geqslant 0$. The limiting case $c = 0$ implies that direct pathways in the X-shaped waveguide are eliminated. By substituting Eq. (14) into Eq. (12), we obtain the transmission amplitudes

$$S_{2-} = bS_{1+} + \sqrt{\gamma}A_2, \quad S_{3-} = bS_{1+} - \sqrt{\gamma}A_2. \tag{15}$$

Hence, an excitation of the second odd dipole mode gives the difference between the outputs

$$T_2 - T_3 = \frac{4\sqrt{c(1-c)\gamma}}{S_{1+}}\mathrm{Im}(A_2), \tag{16}$$

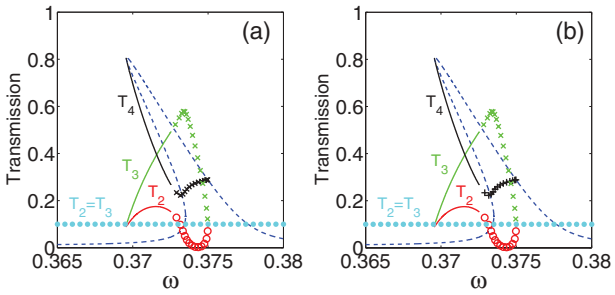


FIG. 7. (Color online) Frequency behavior of light outputs to arms in the X-shaped waveguide for light injects into the first arm with amplitude $S_{1+} = 0.07$ with account of direct path way processes of light transmission from arm 1 into arms 2 and 3 for (a) $c = 0.01$ (weak processes) and (b) $c = 0.1$ (stronger processes). Dashed and dotted lines show the transmission $T_4$ and $T_2 = T_3$ for the symmetry-preserving solution, respectively. Solid red line and open circles (dashed-dotted line and crosses) show the transmission to arm 2 (3). Thicker dashed and dotted lines show the the domains of stability of the symmetry-preserving solution. Open circles and crosses mark the domains of stability of the symmetry-breaking solution.

which is substantial compared to the direct pathway processes proportional to $c$ if $|c| \ll 1$. Figure 7 demonstrates that effect. One can see that for the symmetry-preserving solution, the direct transmission from the input arm 1 into arms 2 and 3 is small, proportional to the small parameter $c$, while for the symmetry-breaking solution inspired by excitation of the odd dipole mode $A_2$, cross talk is rather large where the difference between outputs 2 and 3 is proportional to $\sqrt{c}$.

### D. Light injection into all four arms

Let now light be applied to all four arms with equal power, but amplitudes are opposite in sign: $S_{1+} = -S_{2+} = S_{3+} = -S_{4+} = 0.03$. Then, even in the linear case both dipole modes would be excited. For the nonlinear case, there is the symmetry-preserving solution with $S_{1-} = -S_{2-} = S_{3-} = -S_{4-}$ too as shown in Fig. 8(a). However, there is also the symmetry-breaking solution which gives rise to nonequal outputs. Moreover, for some frequency and for some input power, the outputs to the selected arm might be completely blocked as Fig. 8 shows.

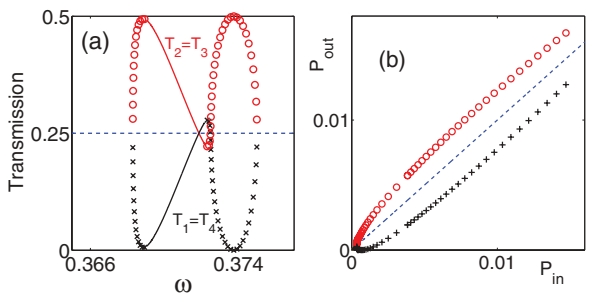


FIG. 8. (Color online) (a) Frequency behavior of transmissions to arms 1, 2, 3, 4 for equal input power $S_{1+} = -S_{2+} = S_{3+} = -S_{4+}$. (b) Output-input curves for fixed frequency $\omega = 0.374$. Dashed blue line marks the symmetry-preserving solution with $T_1 = T_2 = T_3 = T_4$. Open circles and crosses mark the symmetry-breaking solution with $T_1 = T_4$ and $T_2 = T_3$, respectively.

## III. CROSS TALK IN PHOTONIC CRYSTAL X-SHAPED WAVEGUIDE

In this section, we present the solution of the Maxwell equations which describe propagation of the TM mode in the PhC X-shaped waveguide with nonlinear dipole defect cavity. Figure 1 shows two degenerated solutions for the closed defect cavity. The parameters of the rods as well as of the PhC structure are given in Fig. 1. Next, we open the defect by removal of the rods marked by dashed open circles to obtain the X-shaped waveguide that holds the nonlinear defect rod. Then, the dipole eigenmodes decay into the arms of the waveguide.

In order to solve a scattering problem in the PhC X- and T-shaped waveguides with single nonlinear dipole defect, we use here the approaches borrowed from electron quantum transport.[29–31] Basically, they reduce the problem onto a space covering only the scattering region without infinite length waveguides by use of non-Hermitian effective Hamiltonian $H_{\text{eff}}$. Then, the scattering wave function $|\psi_S\rangle$ within the scattering region obeys the equation

$$(H_{\text{eff}} - E)|\psi_S\rangle = V|E, L\rangle, \tag{17}$$

which is the form of the Lippmann-Schwinger equation.[31] Here, $E$ is the energy of incident electron, $|E, L\rangle$ are known extended states of the $L$th waveguide, and the matrix $V$ is responsible for coupling of inner states with incoming waves over the waveguides. For electronic transport, these states are well-known analytic solutions. As a result, the effective Hamiltonian $H_{\text{eff}}$ can be found analytically.[29–31]

If we were to consider to the PhC waveguides coupled with defects, the approach is to be modified because the waveguide Bloch modes are accessible only numerically. Details of the numerical procedure to calculate the solution of the nonlinear Maxwell equations are given in the Appendix. The procedure is a self-consistent solution of the system of nonlinear equations for those points that belong to the nonlinear defect rod. In contrast from the monopole mode of the pointlike nonlinear defect,[19] the dipole modes undergo a swap variation in the interior of the defect as seen from Fig. 1. Therefore, the number of sites in the interior of the nonlinear defect should be large enough in order to describe the solution within the dipole defect rod. To be specific, we used the $40 \times 40$ numerical grid per elementary cell. Respectively, the defect rod was meshed into around 200 sites.

Figures 9(a) and 9(b) show the transmissions when light is injected into arm 1 for two different designs of the dipole nonlinear defect. In the Fig. 9(a), the defect is hidden among eight auxiliary linear rods as shown in Fig. 10. Then, the coupling of the defect cavity with waves in the arms is small and the direct pathway processes are almost canceled. In Fig. 9(b), the defect rod has larger coupling with the X-shaped waveguide. The direct path processes of light propagation in the waveguide are allowed. As a result, in the solution in which both dipole modes are excited, one can observe the symmetry breaking for the cross talking, i.e., $T_2 \neq T_3$. That result is shown in Fig. 9(b) by dashed-dotted and

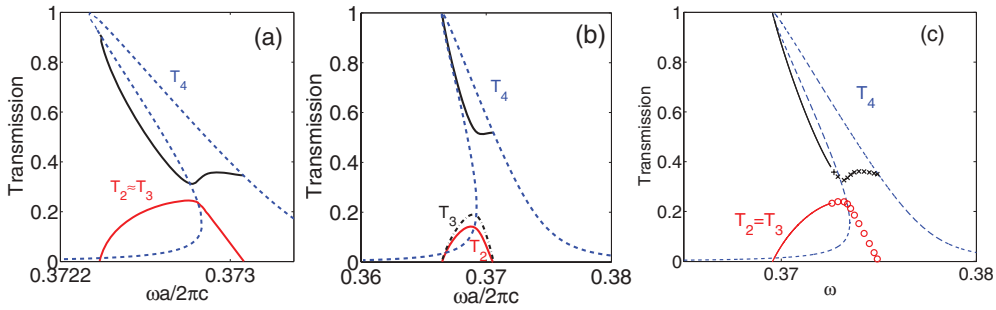


FIG. 9. (Color online) Frequency behavior of light outputs to arms for light injects into the first arm. (a) Dipole defect is hidden with input power $P = 0.1W/a$. (b) Defect is opened as shown in Fig. 10 with $P = 1W/a$. Dashed blue line shows the transmission $T_4$ when only the even dipole mode $E_1$ is excited, solid blue line shows $T_4$, dashed-dotted black line shows $T_2$, and solid red line shows $T_3$ when both dipole modes are excited. (c) The CMT-based transmission [see Fig. 2(b)].

solid lines. Figure 9(c) copies Fig. 2(b) in order that the reader could compare the results of direct computation of the Maxwell equations described in the Appendix with the model CMT results when the direct path processes are excluded. One can see good quantitative agreement between two approaches.

For illustration of the direct path processes and the symmetry-breaking effect, we computed the streamlines by use of the streamline function.[32] One can see from Fig. 10(a) that light follows in a laminar way from input arm 1 to output arm 4. And, there are no the streamlines to the cross arms 2 and 3 as shown in Fig. 10(a) for the solution with the first even dipole mode excited only. Figure 10(b) shows the second solution of the Maxwell equations when both dipole modes are excited due to the Kerr effect. In the vicinity of the dipole defect, the solution becomes superposed of both dipole modes to give rise to an optical vortex[24] that is seen as closed circular streamlines around the defect. There are also streamlines which go to cross arms 3 and 4 that demonstrate the cross talk phenomenon. However, there is no symmetry breaking in respect to cross outgoing waves.

In the second design, due to a removal of 16 linear rods around the nonlinear defect rod, we have a substantial direct path transmission from arm 1 into arms 2 and 3 as Fig. 11(a) demonstrates for the solution with the only even dipole mode excited. That takes place irrespective of whether the dipole defect is linear or not. Similar to the case shown in Fig. 10(b), there is the solution of the Maxwell equations with both dipole modes excited shown in Fig. 11(b). In agreement with the CMT [see Eq. (16), the transmissions to cross arms 2 and 3 become different, i.e., symmetry breaking occurs. This phenomenon is demonstrated in Fig. 11(b) by streamlines and the real part of the solution. There are two equivalent solutions with either $T_2 > T_3$ or $T_2 < T_3$, which can be switched between by pulses of input light.[17,33]

The next figures present the case when light is injected into two arms simultaneously. Figure 12 shows the solutions of the Maxwell equations when light is injected to arms 1 and 2. It is clear that for the linear defect, both dipole modes would be excited equally. The solution of the Maxwell equations with the nonlinear dipole defect shows the similar result as shown in Fig. 12(a). However, as opposed to the linear case there might be solutions where dipole modes are excited with different amplitudes. That gives rise to the symmetry breaking with respect to the outputs 3 and 4. In the case $S_{1+} = S_{4+}$ as it follows from Eq. (7), the dipole modes are not excited at all to give rise to total reflection of the injected light as shown in Fig. 13(a) . In this case, the solution is real (standing wave) with accuracy up to a small contribution from direct path processes. If the injected light amplitudes are opposite in sign, the solution is also standing wave in the vicinity of the dipole defect. Then, for the solution with only one dipole excited, cross talk is eliminated. For the solution with both dipole modes excited, light propagates into arms 2 and 3 to allow cross talk as shown in Fig. 13(b). We also calculated the

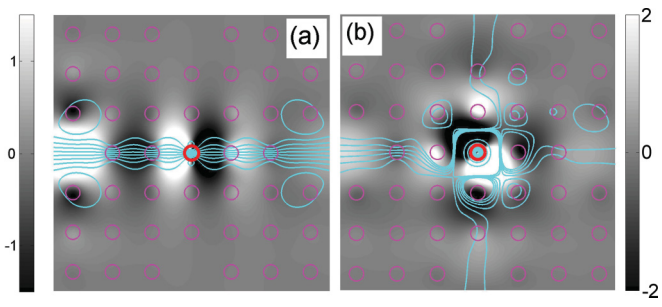


FIG. 10. (Color online) Real part of the solutions ($z$ component of electric field) of the Maxwell equations for light injects into the first arm with fixed input power $P = 0.1W/a$ and fixed frequency $\omega a/2\pi = 0.3728$. Dielectric rods which form the PhC waveguide are shown by pink open circles. The dipole defect is shown by red bold open circle. Light blue lines show the optical streamlines. (a) The solution with the only even dipole mode excited. (b) Another solution with both dipole modes excited.

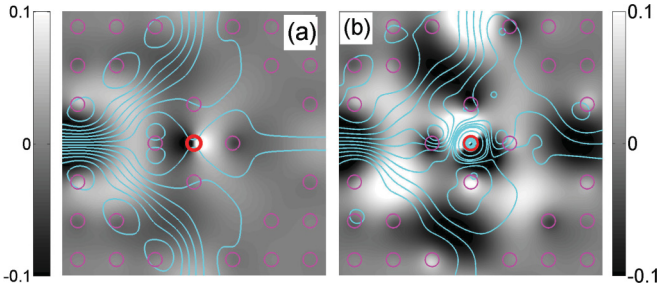


FIG. 11. (Color online) The same as in Fig. 10, but the dipole defect is opened with $P = 1W/a$ and $\omega a/2\pi = 0.37$.

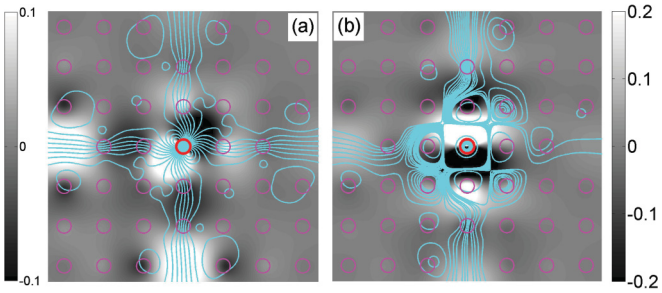


FIG. 12. (Color online) Real part of the solutions of the Maxwell equations for light injects into the first and second arms with fixed input power $P = 0.1W/a$ and $\omega a/2\pi = 0.3728$. (a) The symmetry-preserving solution and (b) the symmetry-breaking solution.

solutions of the Maxwell equations when the light is injected into three and four arms simultaneously. The results are in good agreement with the solutions obtained by the CMT (Sec. II).

## IV. ALL-OPTICAL SWITCHING IN T-SHAPED WAVEGUIDE

The T-shaped waveguide three-port system is currently studied in the context of channel-drop filter.[1,26,34–37] In Ref. 12, two nonlinear monopole defects symmetrically positioned in the T-shaped PhC waveguide were considered. It was shown that the symmetry breaking may occur due to the nonlinearity with almost full blocking of light transmission into one of the arms.[12] Pulses of light switch the transmission from one arm into another.[33]

Here, we consider the single dipole defect in the T-shaped waveguide shown Fig. 14. We will show that the waveguide can be switched from the regime of full blocking of light outputs to the regime of cross talk. We choose two different positions of the nonlinear dipole defect in the waveguide as shown in Fig. 14, the centered position [Figs. 14(a) and 14(b)] and the shifted position [Figs. 14(c) and 14(d)]. The CMT equations are similar to Eqs. (2), (7), and (9) and take the following form for the shifted position:

$$D = \begin{pmatrix} \sqrt{\gamma_1} & 0 \\ \sqrt{\gamma_2} & \sqrt{\gamma_3} \\ \sqrt{\gamma_2} & -\sqrt{\gamma_3} \end{pmatrix}, \quad \hat{\Gamma} = D^{+}D/2 = \begin{pmatrix} \frac{1}{2}\gamma_1 + \gamma_2 & 0 \\ 0 & \gamma_3 \end{pmatrix}, \tag{18}$$

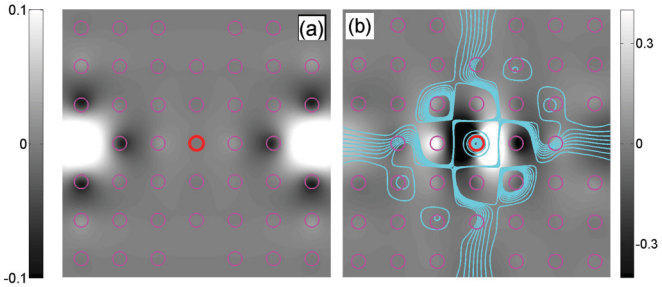


FIG. 13. (Color online) Real part of the solutions of the Maxwell equations for light injects into the 1 and 4 arms with (a) the equaled amplitudes $S_{1+} = S_{4+}$. (b) Both dipole modes are excited for the case $S_{1+} = -S_{4+}$ to give rise to cross talk. The input power per length $P = 0.1W/a$ and the frequency $\omega a/2\pi = 0.3728$.

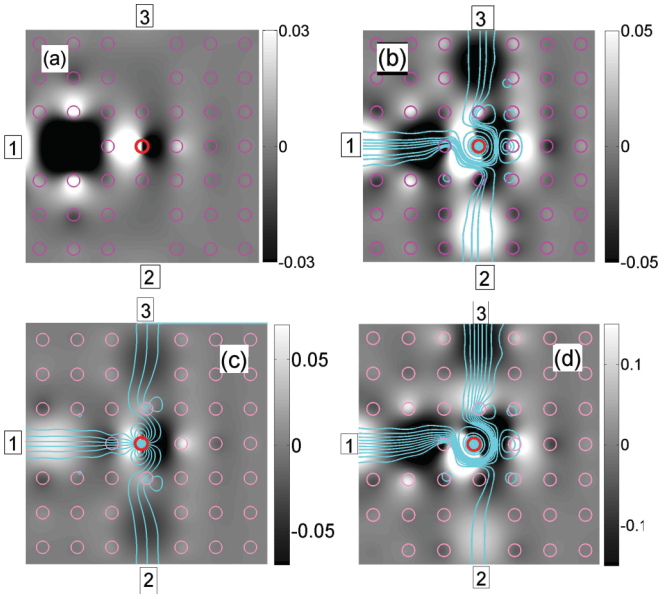


FIG. 14. (Color online) Real part of the solutions of the Maxwell equations in the T-shaped waveguide with single nonlinear dipole defect for $\omega a/2\pi c = 0.368$ and $P = 1W/a$. (a) The symmetry-preserving solution and (b) the symmetry-breaking solution for the nonlinear dipole defect at the center of the waveguide. (c) The symmetry-preserving solution and (d) the symmetry-breaking solution for the nonlinear dipole defect shifted by a distance $d = 0.15a$.

$$\begin{aligned} &[\omega - \omega_0 + \lambda_{11}|A_1|^2 + \lambda_{12}|A_2|^2 + \frac{i}{2}\gamma_1 + i\gamma_2]A_1 \\ &\quad + 2\lambda_{12}\mathrm{Re}(A_1^* A_2)A_2 = i\sqrt{\gamma_1}S_{1+} + i\sqrt{\gamma_2}(S_{2+} + S_{3+}), \\ &2\lambda_{12}\mathrm{Re}(A_1^* A_2)A_1 + [\omega - \omega_0 + \lambda_{22}|A_2|^2 + \lambda_{12}|A_1|^2 + i\gamma_3]A_2 \\ &\quad = i\sqrt{\gamma_3}(S_{2+} - S_{3+}), \end{aligned} \tag{19}$$

$$\begin{aligned} S_{1-} &= -S_{1+} + \sqrt{\gamma_1}A_1, \\ S_{2-} &= -S_{2+} + \sqrt{\gamma_2}A_1 + \sqrt{\gamma_3}A_2, \\ S_{3-} &= -S_{3+} + \sqrt{\gamma_2}A_1 - \sqrt{\gamma_3}A_2. \end{aligned} \tag{20}$$

Here, $\sqrt{\gamma_1}$ is the coupling constant of the first dipole mode $E_1(x,y)$ with wave in the central arm 1, $\sqrt{\gamma_2}$ is the coupling constant of that mode with wave in the aside arms 2 and 3, $\pm\sqrt{\gamma_3}$ is the coupling constant of the second dipole mode $E_2(x,y)$ with waves in arm 2 or 3, respectively. For the centered position of the defect, we would have $\gamma_1 = \gamma_3$, $\gamma_2 = 0$. By the same procedure used for the X-shaped waveguide, we obtained $\gamma_1 = \gamma_3 = 0.00075$, $\gamma_2 = 0$ for the centered position of the dipole defect, and $\gamma_1 = 0.00073$, $\gamma_3 = 0.0007$, $\gamma_2 = 0.00025$ in terms of $2\pi c/a$.

In what follows, we consider that light injects into the central arm 1 and transmits into the cross arms (enumerated 2 and 3), i.e., $S_{2+} = S_{3+} = 0$. For the centered position of the dipole defect, there are two regimes of processing of the dipole defect. In the first one, the even dipole mode is only excited. When $\gamma_2 = 0$, there is no light outgoing into the cross arms. Therefore, in that regime the centered nonlinear dipole defect blocks light transmission as shown by dashed lines in Fig. 15(a). In the second regime of the nonlinear dipole

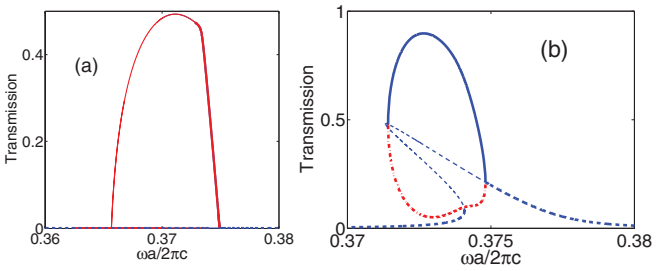


FIG. 15. (Color online) Transmission from the left central arm to the down and up arms in the T-shaped waveguide holding a single nonlinear dipole defect for $S_{1+} = 0.05$. (a) The defect is not shifted and (b) the defect is shifted by a distance $d = 0.15a$. Dashed line shows the symmetry-preserving solution. Solid line shows the transmission to the down arm and dashed-dotted line shows the transmission to the up arm for the symmetry-breaking solution.

defect processing, both dipole modes are excited. That opens the waveguide as shown in Fig. 15(a) by the solid line. The light transmission for the shifted position of the dipole defect in the T-shaped waveguide is presented in Fig. 15(b). There are also two solutions, but both with cross talk. The first symmetry-preserving solution has equal outputs, while the second solution breaks the symmetry with different outputs into the cross arms. Figure 15(b) demonstrates a profound asymmetry of light outputs.

The results of the CMT qualitatively agree with the numerical solutions of the Maxwell equations shown in Fig. 14. In particular, Fig. 14(a) shows that the solution is a standing wave for the only first dipole mode excited. The Poynting current equals zero. As a result, there are no optical streamlines in that solution. In the second solution of the Maxwell equations, both dipole modes are excited to give rise to the streamlines from the input arm to the cross arms, i.e., cross talk as shown in Fig. 14(b). In the second design of the T-shaped waveguide, there are also two solutions of the Maxwell equations presented in Figs. 14(c) and 14(d). For the first symmetry-preserving solution, the first dipole mode is excited only. However, because of coupling of the dipole mode with waves in all arms, cross talk takes place as streamlines demonstrate in Fig. 14(c). For the symmetry-breaking solution, there is asymmetry of light outputs in the cross arms as seen in Fig. 14(d).

## V. SUMMARIES AND CONCLUSIONS

We considered light transmission in the linear PhC X- and T-shaped waveguides with a single nonlinear defect made from a Kerr medium. We assumed that among all eigenmodes of the defect optical cavity, only two degenerated dipole modes fall into the propagation band of the waveguides. When the dipole defect positioned at the center of the X-shaped waveguide is linear, light transmission would be only directional. In other words, cross talk would be eliminated as was first noted by Johnson *et al.*[2] In the case of the T-shaped waveguide, we would have full reflection of light injected into the central arm. For the nonlinear case, these statements are still correct. There is a stable solution of nonlinear CMT equations where a wave injected into the central arm excites only the dipole mode with the parity of the injected wave while the second dipole mode with opposite parity remains dark. We have shown that there is another stable solution where both dipole modes are excited because of nonlinear terms in the CMT equations. As a result, cross talk occurs in the waveguides. This results is in good agreement with solutions of the Maxwell equations for the PhC X- and T-shaped waveguides.

The above mentioned refers to the well-hidden dipole defect when the direct path propagation of light in the waveguides is negligible. Then, for the second solution where both dipole modes participate in the resonant transmission, the odd dipole mode emits into the cross arm waves opposite in sign. When the dipole defect is opened, the direct path process takes place. These processes interfere with outgoing waves $S_{2-} = -S_{3-}$ resonantly transmitted by the dipole defect. This immediately gives rise to the symmetry breaking in the cross outputs. The phenomenon was found both in the solution in the CMT equations and in the numerical solution of the Maxwell equations. Thus, in view of these phenomena, single nonlinear dipole defect in the linear waveguides opens a wide spectrum of possibilities to manipulate light propagation in the X- and T-shaped waveguides.

## ACKNOWLEDGMENTS

The work is partially supported by Integration Project of Siberian Branch of RAS (Project No. 29) and RFBR Grant No. 12-02-000094. We thank D. N. Maksimov for critical reading of the manuscript.

## APPENDIX

For computations, we follow the paper by Rahachou and Zozoulenko[38] where a tight-binding Hamiltonian $\hat{H}$ at the numerical grid $(m,n)$ was formulated to solve numerically the Maxwell equations:

$$\hat{H}|f\rangle = (\omega\Delta/c)^2|f\rangle, \tag{A1}$$

where for the TM modes

$$f_{mn} = \sqrt{\epsilon_{mn}}E_{mn}. \tag{A2}$$

The tight-binding Hamiltonian has a standard form with diagonal matrix elements $4/\epsilon_{mn}$, and the matrix elements which are responsible for the next-nearest neighbor equal $-\frac{1}{\sqrt{\epsilon_{mn}}}\frac{1}{\sqrt{\epsilon_{(m,n)+\mu}}}$. Here, $\epsilon_{mn}$ and $E_{mn}$ are the dielectric constant and the $z$ component of electric field mapped onto the numerical grid shown in Fig. 16. The total area of the scattering region is $M \times N$.

At each vertical slice $m$, we define the state $\Psi_m$ consisting of $f_{m1}, f_{m2}, \ldots, f_{m,N}$. The TM mode incident from the left (shown by arrow in Fig. 16) is

$$\Psi_m^\alpha = \exp(ik_\alpha m\Delta)\Phi_m^\alpha, \tag{A3}$$

where $k_\alpha$ is the Bloch vector directed along the waveguide and $\Phi_m$ is the Bloch state at the slice $m$. Respectively, the reflected and transmitted states can be written as follows:

$$\Psi_m = \sum_\beta t_{\beta\alpha}\exp[ik_\beta(m-M-1)\Delta]\Phi_m^\beta, \quad m \geqslant M \tag{A4}$$

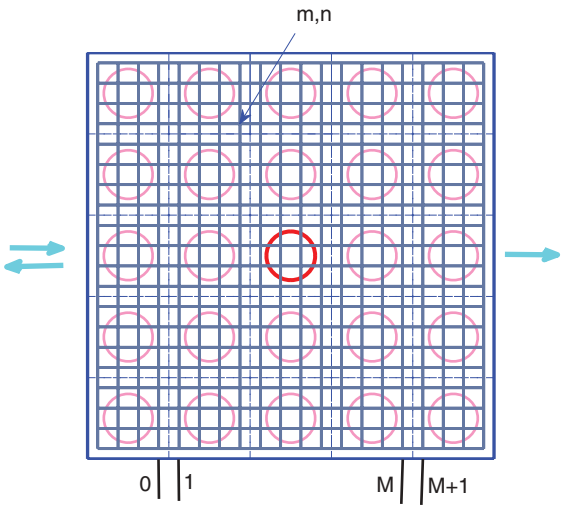


FIG. 16. (Color online) Numerical grid shown by gray solid lines. Green dashed lines show PhC elementary cells. $P = a_0/\Delta$ is the number of slices per the elementary unit.

$$\Psi_m = \sum_\beta r_{\beta\alpha} \exp(-ik_\beta m\Delta)\Phi^\beta_{1-m}, \quad m \leqslant 1 \tag{A5}$$

where $r_{\beta\alpha}$ and $t_{\beta\alpha}$ are the reflection and transmission amplitudes, respectively. The Bloch states are periodical with the period $P$, i.e., $\Phi^{(\alpha)}_m = \Phi^{(\alpha)}_{m+P}$.

Maxwell equations (A1) are an infinite set of algebraic equations. However, we can restrict them by using that the solutions in the waveguides are known numerically. From Eq. (A4) follows

$$\Psi_{M+1} = \hat\Phi_{M+1}\hat t = \hat\Phi_1\hat t, \quad \Psi_M = \hat\Phi_0\hat K^{-1}\hat t, \tag{A6}$$

where $\hat t = t_{\beta\alpha}$ and $(\hat\Phi_m)_{n\alpha} = \Phi^\alpha_{mn}$ is a squared matrix $N \times N$, and $\hat K = \delta_{\alpha\beta}\exp(ik_\alpha\Delta)$. Then, we have

$$\Psi_{M+1} = \hat\Phi_1\hat K\hat\Phi_0^{-1}\Psi_M. \tag{A7}$$

This equation couples the solution at the nearest slice $M$ and the solution at the slice $M+1$ at the right waveguide.

From Eq. (A5), we have at the left waveguide

$$\Psi_0 = \hat\Phi^{(1)}_0 + \hat\Phi_1\hat r, \quad \Psi_1 = \hat\Phi^{(1)}_1 e^{ik_1\Delta} + \hat\Psi_0\hat K^{-1}\hat r. \tag{A8}$$

Here, the upper index (1) implies that the incoming light has $\alpha = 1$. Next, we obtain from Eq. (A8)

$$\Psi_0 = \hat\Phi_1\hat K\hat\Phi_0{}^{-1}\Psi_1 + \left[\hat\Phi^{(1)}_1 - \hat\Phi_1\hat K\hat\Phi_0^{-1}\hat\Phi^{(1)}_1 e^{ik_1\Delta}\right]. \tag{A9}$$

From these equations, we can express the reflection amplitudes matrix as

$$\hat r = \hat K\hat\Phi_0^{-1}\left[\Psi_1 - \hat\Phi^{(1)}_1\exp(ik_1\Delta)\right]. \tag{A10}$$

Equations (A7) and (A9) allow us to formulate the closed system of equations.

Thus, we express Eq. (A1) in the form of the Lippmann-Schwinger equation (17):

$$[\hat H^{(\mathrm{eff})} - (\omega\Delta/c)^2]|\Psi_S\rangle = |S^{(\mathrm{in})}\rangle, \tag{A11}$$

where the matrix elements of the effective operator

$$\hat H^{\mathrm{eff}}_{mm',nn'} = \hat H_{mm',nn'} - \left(\hat\Phi_1\hat K\hat\Phi_0^{-1}\right)_{nn'}\delta_{Mm}\delta_{Mm'} - \left(\hat\Phi_1\hat K\hat\Phi_0^{-1}\right)_{nn'}\delta_{1m}\delta_{1m'}. \tag{A12}$$

Moreover,

$$S^{(\mathrm{in})}_{mn} = \delta_{1m}\left[\hat\Phi^{(1)}_0 - \hat\Phi_1\hat K\hat\Phi_0^{-1}\hat\Phi^{(1)}_1\exp(ik_1\Delta)\right]_n. \tag{A13}$$

The nonlinear contributions in the basic equation (A1) are given by

$$\epsilon_{mn} = \epsilon_0 + \kappa|E_{mn}|^2, \tag{A14}$$

where $\kappa = \frac{n_0cn_2}{4\pi}$ with accordance to Eq. (5). From Eq. (A2) we have

$$\epsilon_{mn} = \tfrac{1}{2}[\epsilon_0 + \sqrt{\epsilon_0^2 + 4\kappa|f_{mn}|^2}]. \tag{A15}$$

Thus, we finally obtain the system of $N \times M$ nonlinear algebraic equations, which were solved numerically.


[1] J. Joannopoulos, S. G. Johnson, J. N. Winn, and R. D. Meade, *Photonic Crystals: Molding the Flow of Light* (Princeton University Press, Princeton, NJ, 2008).
[2] S. G. Johnson, C. Manolatou, Sh. Fan, P. R. Villeneuve, J. D. Joannopoulos, and H. A. Haus, Opt. Lett. **23**, 1855 (1998).
[3] M. Haelterman and P. Mandel, Opt. Lett. **15**, 1412 (1990).
[4] T. Peschel, U. Peschel, and F. Lederer, Phys. Rev. A **50**, 5153 (1994).
[5] I. V. Babushkin, Yu. A. Logvin, and N. A. Loĭko, Quantum Electron. **28**, 104 (1998).
[6] J. P. Torres, J. Boyce, and R. Y. Chiao, Phys. Rev. Lett. **83**, 4293 (1999).
[7] L. Longchambon, N. Treps, T. Coudreau, J. Laurat, and C. Fabre, Opt. Lett. **30**, 284 (2005).
[8] P. G. Kevrekidis, Zh. Chen, B. A. Malomed, D. J. Frantzeskakis, and M. I. Weinstein, Phys. Lett. A **340**, 275 (2005).
[9] S. Shwartz, R. Weil, M. Segev, E. Lakin, E. Zolotoyabko, V. M. Menon, S. R. Forrest, and U. El-Hanany, Opt. Express **14**, 9385 (2006).
[10] K. Aydin, I. M. Pryce, and H. A. Atwater, Opt. Express **18**, 13407 (2010).
[11] S. Yu, X. Piao, S. Koo, J. H. Shin, S. H. Lee, B. Min, and N. Park, Opt. Express **19**, 25500 (2011).
[12] E. Bulgakov and A. Sadreev, Phys. Rev. B **84**, 155304 (2011).
[13] E. A. Ostrovskaya, Yu. S. Kivshar, M. Lisak, B. Hall, F. Cattani, and D. Anderson, Phys. Rev. A **61**, 031601 (2000).
[14] N. Akhmediev and A. Ankiewicz, Phys. Rev. Lett. **70**, 2395 (1993).
[15] R. Tasgal and B. A. Malomed, Phys. Scr. **60**, 418 (1999).
[16] A. Gubeskys and B. A. Malomed, Eur. Phys. J. D **28**, 283 (2004).
[17] B. Maes, M. Soljaĉić, J. D. Joannopoulos, P. Bienstman, R. Baets, S.-P. Gorza and M. Haelterman, Opt. Express **14**, 10678 (2006).
[18] B. Maes, P. Bienstman, and R. Baets, Opt. Express **16**, 3069 (2008).
[19] E. Bulgakov, K. Pichugin, and A. Sadreev, Phys. Rev. B **83**, 045109 (2011).
[20] V. A. Brazhnyi and B. A. Malomed, Phys. Rev. A **83**, 053844 (2011).

[21]M. F. Yanik, S. Fan, M. Soljačić, and J. D. Joannopoulos, Opt. Lett. **28**, 2506 (2003).
[22]K. Busch, S. F. Mingaleev, A. Garcia-Martin, M. Schillinger, and D. Hermann, J. Phys.: Condens. Matter **15**, R1233 (2003).
[23]A. F. Sadreev, Phys. Rev. E **70**, 016208 (2004).
[24]E. N. Bulgakov and A. F. Sadreev, Phys. Rev. B **85**, 165305 (2012).
[25]W. Suh, Z. Wang, and S. Fan, IEEE J. Quantum Electron. **40**, 1511 (2004).
[26]M. Soljačić, C. Luo, J. D. Joannopoulos, and S. Fan, Opt. Lett. **28**, 637 (2003).
[27]J. Bravo-Abad, S. A. Rodriguez, P. Bermel, S. G. Johnson, J. D. Joannopoulos, and M. Soljaĉić, Opt. Express **15**, 16161 (2007).
[28]H. M. Gibbs, *Optical Bistability: Controlling Light with Light* (Academic, New York, 1985).
[29]T. Ando, Phys. Rev. B **44**, 8017 (1991).
[30]S. Datta, *Electronic Transport in Mesoscopic Systems* (Cambridge University Press, Cambridge, England, 1995).
[31]A. F. Sadreev and I. Rotter, J. Phys. A: Math. Gen. **36**, 11413 (2003).
[32]C. F. Chien and R. V. Waterhouse, J. Acoust. Soc. Am. **101**, 705 (1997).
[33]E. Bulgakov and A. Sadreev, J. Phys.: Condens. Matter **23**, 315303 (2011).
[34]S. Noda, A. Chutinan, and M. Imada, Nature (London) **407**, 608 (2000).
[35]S. Kim, I. Park, H. Lim, and C.-S. Kee, Opt. Express **12**, 5518 (2004).
[36]B.-S. Song, T. Asano, Y. Akahane, and S. Noda, Phys. Rev. B **71**, 195101 (2005).
[37]H. Ren, C. Jiang, W. Hu, M. Gao, and J. Wang, Opt. Express **14**, 2446 (2006).
[38]A. I. Rahachou and I. V. Zozoulenko, Phys. Rev. B **72**, 155117 (2005).